Journal of Chromatography A, 1217 (2010) 6115–6121

Contents lists available at ScienceDirect

Journal of Chromatography A

journal homepage: www.elsevier.com/locate/chroma

Molecularly imprinted magnetic nanoparticles as tunable stationary phase located in microfluidic channel for enantioseparation

Ping Qu, Jianping Lei, Lei Zhang, Ruizhuo Ouyang, Huangxian Ju*

Key Laboratory of Analytical Chemistry for Life Science (Ministry of Education of China), Department of Chemistry, Nanjing University, Nanjing 210093, China

ARTICLE INFO

Article history:
Received 10 May 2010
Received in revised form 19 July 2010
Accepted 23 July 2010
Available online 1 August 2010

Keywords:
Capillary electrochromatography
Enantioseparation
Molecularly imprinted polymer
Magnetic nanoparticles
Tunable stationary phase
Microfluidics

ABSTRACT

A microfluidic device integrated with molecularly imprinted magnetic nanoparticles as stationary phase was designed for rapid enantioseparation by capillary electrochromatography. The nanoparticles were synthesized by the co-polymerization of methacrylic acid and ethylene glycol dimethacrylate on 3-(methacryloyloxy)propyltrimethoxysilane-functionalized magnetic nanoparticles (25-nm diameter) in the presence of template molecule, and characterized with infrared spectroscopy, thermal gravimetric analysis, and transmission electron microscope. The imprinted nanoparticles (200-nm diameter) could be localized as stationary phase in the microchannel of microfluidic device with the tunable packing length by the help of an external magnetic field. Using S-ofloxacin as the template molecule, the preparation of imprinted nanoparticles, the composition and pH of mobile phase, and the separation voltage were optimized to obtain baseline separation of ofloxacin enantiomers within 195 s. The analytical performance could be conveniently improved by varying the packing length of nanoparticles zone, showing an advantage over the conventional packed capillary electrochromatography. The linear ranges for amperometric detection of the enantiomers using carbon fiber microdisk electrode at +1.0 V (vs. Ag/AgCl) were from 1.0 to 500 μM and 5.0 to 500 μM with the detection limits of 0.4 and 2.0 μM, respectively. The magnetically tunable microfluidic device could be expanded to localize more than one kind of template-imprinted magnetic nanoparticles for realizing simultaneous analysis of different kinds of chiral compounds.

1. Introduction

Molecularly imprinted polymers (MIPs) have been widely used as artificial antibodies or enzymes in biosensing [1–5], catalysis [6], extraction [7], separation [8–13], and drug delivery [14,15] due to their stability, ease of preparation, low cost, and specific recognition to the target molecules. However, they often suffer from some drawbacks, such as poor mass transfer, low binding capacity, and slow binding kinetics. Nanosized molecular imprinted materials [16], such as MIP nanoparticles [17,18], nanocapsules [19], nanowires [20] and nanotubes [21,22], are expected to improve the removal of template molecules, the binding capacity and kinetics due to their small dimension and high surface-to-volume ratio. Especially, when combining magnetic nanoparticles (MNPs) with MIP, the resulting MIP–MNPs can be the ideal multifunctional candidate for the separation of different drugs at an external magnetic field [23,24]. For example, MIP–MNPs coupled with high performance liquid chromatography (HPLC) have been applied to perform trace analyses of triazines and tetracycline antibiotics [25,26]. However, up to now the MIP–MNPs have not been used to combine with the advantages of microfluidic device (MD) for separation purpose.

Since microfluidic analysis provides a high degree of separation efficiency and short analysis times, it is recognized as a powerful tool for analytical separations. MD coupling with MNPs has been rapidly developed in immunoassay due to its small volume, pre-nominated position and portability [27–32]. For example, a sandwich on-chip immunoassay has been performed using streptavidin-coated magnetic beads as substrate in a poly(dimethylsiloxane) microfluidic channel structure [28]. A magnetic force-based immunoassay has been devised and successfully applied to detect both rabbit and mouse IgG as the model analytes of microfluidic sandwich immunoassay [30]. These methods utilize adequately the advantages of both MD and MNPs, thus showing good analytical performance. However, although the microchip electrochromatography has become an attractive approach for highly efficient separation, only one work has combined the prominent selectivity of MIPs with microchip electrochromatography to develop a MD for the separation of tert-butoxycarbonyl-tryptophan enantiomers [33]. The proposed in situ preparation of MIP-coated microchannel is difficult to control the coat length for improving the separation. Thus, it is significant to employ tunable MIP–MNPs

* Corresponding author. Tel.: +86 25 83593593; fax: +86 25 83593593.
E-mail address: hxju@nju.edu.cn (H. Ju).

0021-9673/$ – see front matter © 2010 Elsevier B.V. All rights reserved.
doi:10.1016/j.chroma.2010.07.063

as stationary phase in the microchannel of MD for enantioseparation.

Enantioselective separation of chiral drugs has been a topic with great attention since the pharmacokinetics and pharmacodynamics differs between the enantiomers of chiral drugs [34]. For example, S-ofloxacin is 8–128 times more potent in inhibiting the multiplication of gram bacteria than R-ofloxacin, and approximately two times more active than the racemic ofloxacin [35]. Several methods for enantioseparation of racemic ofloxacin have been reported, including ligand exchange chromatography [36], capillary electrophoresis [37] and capillary electrochromatography [34]. Although these techniques have shown baseline separation of ofloxacin enantiomers, they are time-consuming (from 10 to 30 min) and have great consumption of reagents and samples.

Here, a MD integrated with MIP–MNPs as magnetically tunable stationary phase (MIP–MNPs–MD) was designed for rapid enantioseparation of ofloxacin enantiomers. The MIP–MNPs were synthesized on functionalized magnetic nanoparticles using S-ofloxacin as the template, methacrylic acid (MAA) as the functional monomer and ethylene glycol dimethacrylate (EDMA) as the cross-linker. By integrating the advantages of MIPs, MNPs and MD, the developed method achieved baseline enantioseparation of ofloxacin enantiomers within 195 s. The designed MIP–MNPs–MD with low cost shows excellent separation efficiency and promising analytical application in enantioseparation.

2. Experimental

2.1. Reagents and materials

Hydroxyl group modified superparamagnetic nanospheres (50 mg mL^{-1}) with the mean diameter of 25 nm were obtained from Kisker (Steinfurt, Germany). Racemic ofloxacin and S-ofloxacin were purchased from Jiangsu Institute for Food and Drug Control (Nanjing, China). 3-(Methacryloyloxy)propyltrimethoxysilane (γ-MPS), MAA, and EDMA were all purchased from Alfa Aesar (Ward Hill, MA, USA). 2,2′-Azobisisobutyronitrile (AIBN) was obtained from Acros (Geel, Belgium). HPLC-grade acetonitrile (ACN) was supplied by Sigma–Aldrich (St. Louis, MO, USA). Fused-silica capillary with an inner diameter (i.d.) of 25 μm and outer diameter (o.d.) of 365 μm was purchased from Yongnian Optic Fiber Plant (Hebei, China). Sylgard 184 silicone elastomer and curing agent were purchased from Dow Corning (Midland, MI, USA). The running buffer and supporting electrolyte for microchip electrochromatographic separation and amperometric detection were a mixture of ACN and acetate buffer solution (Nanjing Chemicals, Nanjing, China) filtered with 0.2 μm membranes. All aqueous solutions were prepared using ≥18 MΩ ultrapure water (Milli-Q, Millipore, USA).

2.2. Equipments

The size and morphology of the nanoparticles were measured by a JEM-200CX transmission electron microscopy (TEM) (JEOL, Japan) operating at an acceleration voltage of 100 kV. Thermal gravimetric analysis (TGA) was conducted on a Shimadzu TGA-50 instrument (Japan) from room temperature to 600 °C with a heating rate of 10 °C min^{-1} in a nitrogen flow (100 mL min^{-1}). Fourier transform infrared (FTIR) spectra were recorded on a Nicolet 400 FTIR spectrometer (Madison, WI, USA). The UV–vis spectra were characterized with UV-3600 UV–vis–NIR spectrophotometer (Shimadzu, Kyoto, Japan). An inverted fluorescence microscope (Nikon Eclipse TE2000-U, Japan) was used to observe the packed length of MIP–MNPs in the microchannel. Ultrasonic disintegrator with a 2-mm-o.d. probe from Ningbo Scientz Biotechnology (Ningbo, China) was used to prepare the sampling fracture on the separation capillary. Microinjection pump (Baoding Longer Precision Pump Co., Ltd., Shanghai, China) was used to operate the syringe. A laboratory-built high-voltage power supply controlled automatically by computer during experiments was used to supply separation voltage between 0 and +5000 V and sampling voltage between 0 and +1000 V, respectively. Electrochemical measurements were performed on a CHI 812 electrochemical station (CH Instruments Co., China). For amperometric detection, a home-made carbon fiber microdisk working electrode was prepared and the detailed description on the preparation procedure was reported elsewhere [33]. A 40 multiple light microscope (Nanjing Optics Instruments Factory, Nanjing, China) was employed to monitor the position of the working electrode.

Table 1
Condition optimization for the preparation of MIP–MNPs.

No. of MIP–MNPs	M/T[a]	C/M[b]	T (°C)	Time (h)	Resolution
1	1:1	3:4	70	6	0.38
2	4:1	3:4	70	6	1.46
3	8:1	3:4	70	6	0.35
4	4:1	1:4	70	6	0.34
5	4:1	3:1	70	6	0.30
6	4:1	3:4	70	3	Single peak
7	4:1	3:4	70	9	Single peak
8	4:1	3:4	50	6	Single peak
9	4:1	3:4	90	6	Single peak
10	No T	3:4	70	6	Single peak

Electrochromatographic conditions: ACN/40 mM acetate buffer (90/10 (v/v), pH 4.0); detection potential, +1.0 V; injection voltage, 200 V for 2 s; separation voltage, 1200 V.

[a] M/T: the molar ratio of functional monomer to template.
[b] C/M: the molar ratio of cross-linker to functional monomer.

2.3. Preparation of MIP–MNPs

The MNPs were first functionalized with γ-MPS by dropwise adding 4 mL of γ-MPS into MNPs (50 mg) dispersed in 1 mL of 1:1 ethanol and water (v/v) and reaction for 12 h at 40 °C under N_2 atmosphere. After separated from the mixture and rinsed with chloroform, the functionalized MNPs were resuspended in chloroform to perform the synthesis of MIP–MNPs in a 100-mL flask equipped with a mechanical stirrer, N_2 atmosphere and cooling with cycled water. The optimization of the synthesis conditions was shown in Table 1. The mixture of S-ofloxacin (0.361 g) and MAA (340 μL) in chloroform was first shaken for 10 h to form a template–monomer complex. 40 mL of chloroform and the functionalized MNP suspension were then added into the complex solution, followed by adding EDMA (566 μL) and AIBN (50 mg). The polymerization reaction was allowed to proceed for 6 h at 70 °C. The resulting product was collected by the external magnetic field and eluted with a mixture solvent of methanol/acetic acid (9:1, v/v) for several times to extract the template molecules until the eluant was free from S-ofloxacin, which was monitored with UV–vis spectrometry at 293 and 329 nm. The obtained MIP–MNPs were finally rinsed with ethanol to remove the remaining acetic acid. As control, non-molecularly imprinted magnetic nanoparticles (NIP–MNPs) were prepared according to the identical manner in the absence of S-ofloxacin.

2.4. Fabrication of MIP–MNPs–MD

First, the slurry of MIP–MNPs was introduced into the capillary (80 mm length) using a syringe with microinjection pump, and packed in a region where the magnets were located, as shown in Fig. 1. The dense MIP–MNPs packing could be used as a stationary support for highly efficient separation. The MIP–MNPs–MD was then prepared according to our previous procedure [38]. Briefly, a

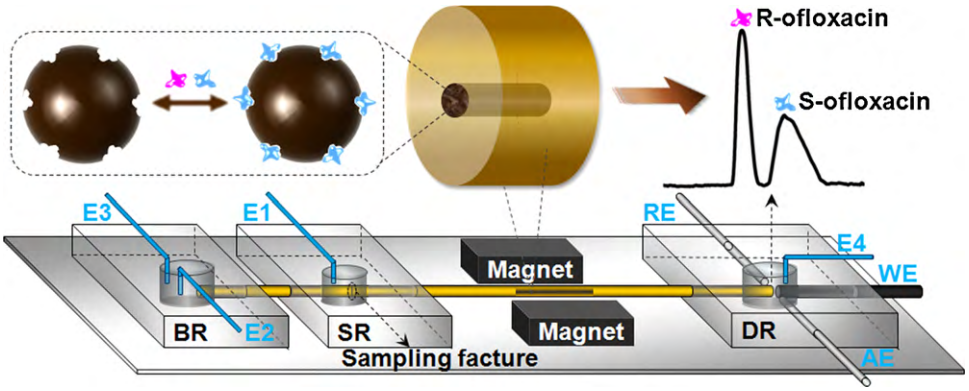

Fig. 1. Schematic representation of enantioseparation on MIP–MNPs–MD. BR, buffer reservoir; SR, sample reservoir; DR, detection reservoir; WE, working electrode; RE, reference electrode; AE, auxiliary electrode; E1, E2, E3 and E4, electrodes for applying sampling and separation voltages.

poly(dimethylsiloxane) matrix with an inner channel of 365-μm diameter was divided into three segments as the polymer retainers for the preparation of buffer reservoir (BR), sampling reservoir (SR), and detection reservoir (DR), respectively. The MIP–MNP packed capillary with two short magnets was then inserted into the SR retainer until a small scratch made previously appeared in the area of SR. After the BR and DR retainers were assembled to the two sides of the SR retainer by the capillary, the sampling fracture was obtained in the SR by sonicating the small scratch. Electrodes E1, E2, E3 and E4 were inserted into SR, BR, BR and SR to achieve the sampling and separation, respectively. The sampling voltage was applied between E1 and E2 with E3 and E4 in floating. The separation voltage was applied between E3 and E4 with E1 and E2 in floating. The voltage of 1000 V was applied to both ends of the capillary for 30 min to increase the packing density and remove the untrapped particles [39,40]. Subsequently, the working electrode was mounted in the guide channel of the DR retainer, exactly opposite to the end of the separation channel at an optimum distance of 15 ± 5 μm [38,41], and an Ag/AgCl reference electrode and a Pt wire as the auxiliary electrode were inserted to two sides of the DR to obtain an integrated three-electrode system for amperometric detection. The resulting MIP–MNPs–MD was shown in Fig. 1.

2.5. Enantioseparation of chiral compounds

The MIP–MNP packed microchannel in the MD was first washed with buffer solution at a voltage of 1000 V. The fracture sampling was then performed by applying an optimum injection voltage of 200 V between the SR and the BR. The separation voltage was finally applied to the BR with the DR grounded and the SR floating by automatically switching the high-voltage contacts, and the electropherogram was recorded on a CHI 812 using the "amperometric *i–t* curve" mode at an applied potential of +1.0 V. All experiments were performed at room temperature. Due to the asymmetric tailing of the peaks, R_s was calculated with the equation: $R_s = (t_{R2} - t_{R1})/(w_1^{1/2} + w_2^{1/2})$ [42,43], where t_{R1} and t_{R2} are the retention time of R-ofloxacin and S-ofloxacin, and $w_1^{1/2}$ and $w_2^{1/2}$ are their adjacent baseline half bandwidths, respectively.

3. Results and discussion

3.1. Characterization of MIP–MNPs

To obtain stable MIP–MNPs, the MNPs were first functionalized with γ-MPS for introducing methacryloyl group on the surface, which could then react with the methacrylate group of EDMA to initiate the co-polymerization of MAA and EDMA on the surface in the presence of AIBN. The FTIR spectra of MNPs, γ-MPS-functionalized MNPs, MIP–MNPs, and MIPs prepared in the absence of MNPs as control were shown Fig. 2A. MNPs, γ-MPS-functionalized MNPs and MIP–MNPs showed obvious Fe–O bond at 586 cm^{-1} (curves a–c) [44]. In comparison of the MNPs and the γ-MPS-functionalized MNPs, the latter showed a band of carbonylic group at 1714 cm^{-1} (curve b), indicative of the presence of methacryloyl group on the surface of MNPs. The MIPs showed the main absorption bands at around 1733, 1257 and 1157 cm^{-1} (curve d), which were assigned to C=O stretching vibration of carboxyl, C–O symmetric and asymmetric stretching vibration of ester, respectively [45]. These absorption bands could be observed from the FTIR spectrum of MIP–MNPs (curve c), confirming the formation of MIPs on the surface.

To confirm the removal of the template molecules after eluting, the UV–vis absorption spectra of the eluants from MIP–MNPs and NIP–MNPs were compared (not shown). The eluant from MIP–MNPs showed the UV–vis absorbance of S-ofloxacin at 293 and 329 nm, which could not be observed in the UV–vis absorption spectrum of the eluant from NIP–MNPs, indicating the efficient elution of template molecules from the as-synthesized MIP–MNPs.

The stability of MIPs was examined with thermal gravimetric analysis. As shown in Fig. 2B, MIP–MNPs showed a small weight loss at the temperatures less than 200 °C. This was attributed to the release of water molecules from the polymer. When the temperature was more than 450 °C, the MIPs were completely decomposed with the weight loss of 100% (curve d), which could also be observed from curve c. The γ-MPS-functionalized MNPs showed a stable weight loss of 12% in the temperature range of 500–600 °C (curve b), which was about 8% more than the MNPs. The latter should result from the decomposition of γ-MPS grafted on MNPs.

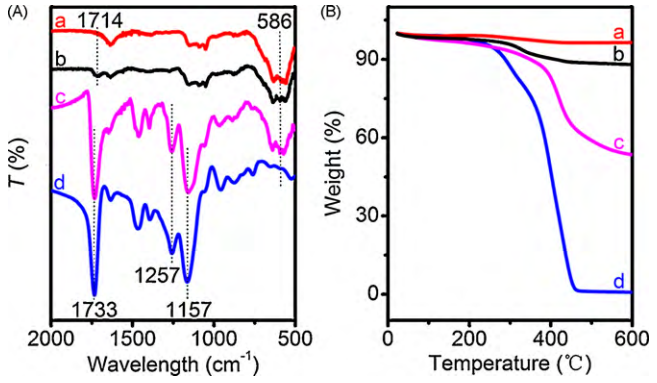

Fig. 2. (A) FTIR spectra and (B) TGA curves of (a) MNPs, (b) γ-MPS-functionalized MNPs, (c) MIP–MNPs, and (d) MIPs.

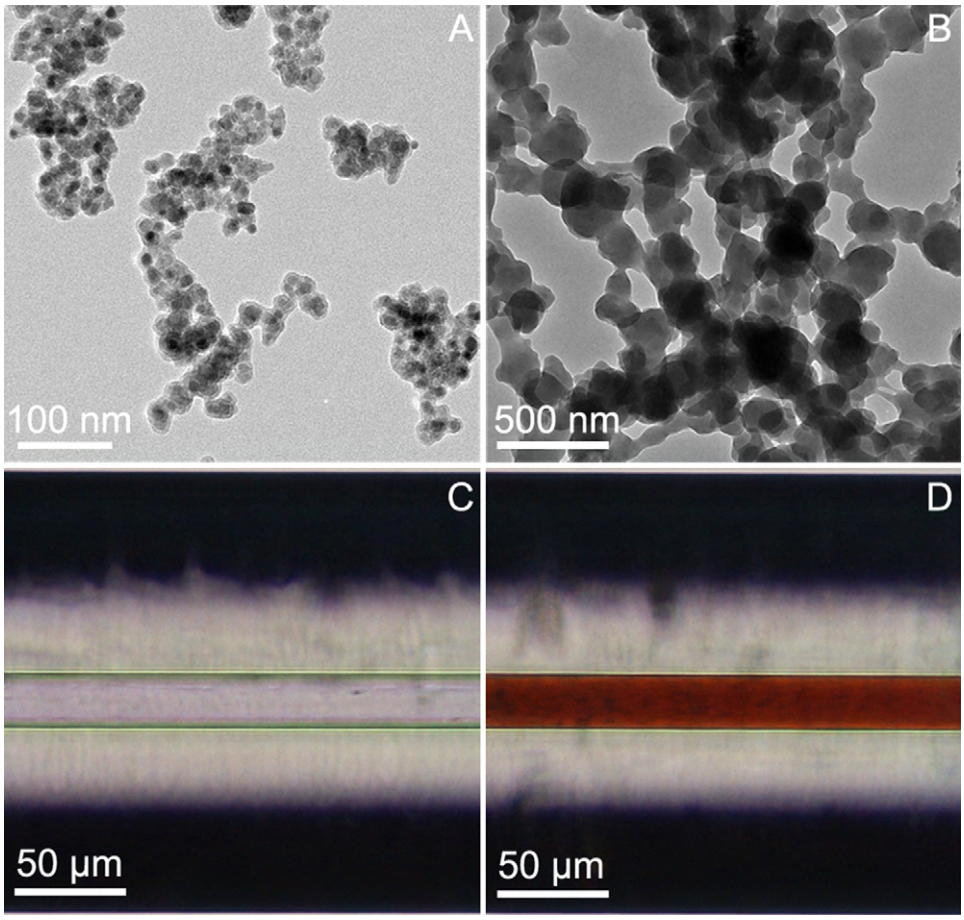

Fig. 3. TEM images of (A) MNPs and (B) MIP–MNPs, and microscopic images of (C) empty capillary and (D) MIP–MNPs located capillary.

The morphological structure of MIP–MNPs could be observed by TEM. Compared with the MNPs, the average diameter of MIP–MNPs increased from about 25 nm of MNPs (Fig. 3A) to about 200 nm (Fig. 3B). The particle size distribution was uniform, which was advantageous of obtaining a permeable and homogeneous packing structure of the MIP–MNPs in the microchannel for highly efficient separation.

3.2. Optimization for the preparation of MIP–MNPs

In order to acquire efficient separation, the synthesis conditions of MIP–MNPs, including the molar ratios of functional monomer to template molecule (M/T) and cross-linker to functional monomer (C/M), and polymerization temperature and time, were optimized. As shown in Table 1, the molar ratios among template molecule, functional monomer and cross-linker affected greatly the resolution due to the changes of the quality of MIPs and the number of recognition sites in the MIPs [46,47]. When the ratio of M/T was 4:1 (No. 2), MIP–MNPs–MD showed the largest resolution of 1.46. Low ratio of M/T (1:1, No. 1) would produce incomplete structure of imprinting cavities, which led to relatively low specificity and the cross-reactivity for R-ofloxacin. However, high ratio (8:1, No. 3) also decreased the resolution due to the insufficient imprinting cavities. The cross-linker could affect the stability and flexibility of recognition cavities. At high cross-linking degree (3:1, No. 5) the recognition ability toward template molecules decreased because it was more difficult for template molecules to enter the cavities of the rigid skeleton. However, high flexibility of MIP skeleton at 1:4 (No. 4) led to low specificity and high cross-reactivity for R-ofloxacin. Thus, the optimal molar ratio of C/M was 3:4 (No. 2), at which the as-prepared MIP–MNPs–MD showed good affinity and specific recognition toward the template S-ofloxacin.

Polymerization temperature and time played important roles in the shape and size distribution of spherical particles [48]. Long polymerization time (9 h, No. 7) or high temperature (90 °C, No. 9) would increase surface thickness and particle size of MIP–MNPs, resulting in low resolution. As polymerization time decreased to 6 h, the resulting MIP–MNPs–MD showed the largest resolution of 1.46 at 60 °C (No. 2) due to the well three-dimensional imprinted cavities coated on MNPs. However, further decreasing the polymerization temperature (3 h, No. 6) or time (50 °C, No. 8) led to a single peak, which could be attributed to less imprinting recognition sites for the enantioseparation.

In addition, the amount of MIPs coated on MNPs should also affect the enantioseparation. To optimize the amount, different volumes of MNPs (0.2, 1.0, and 5.0 mL) were used for the synthesis of MIP–MNPs. At the volume of 5.0 mL, many unreacted MNPs could be observed on the image of TEM (not shown). The optimal volume of MNPs was evaluated to be 1.0 mL for the synthesis of the MIP–MNPs. After optimizing the ratios of C/M/T and other conditions, this method for synthesizing imprinted stationary phase could be applied to other organic template molecules.

3.3. Microscopic images of microchannel and optimization of packing length

The MIP–MNP packed microchannel could be easily prepared only by placing a magnet with tunable length adjacent the microchannel and injecting the MIP–MNP suspension with a microinjection pump into the microchannel. Compared with the

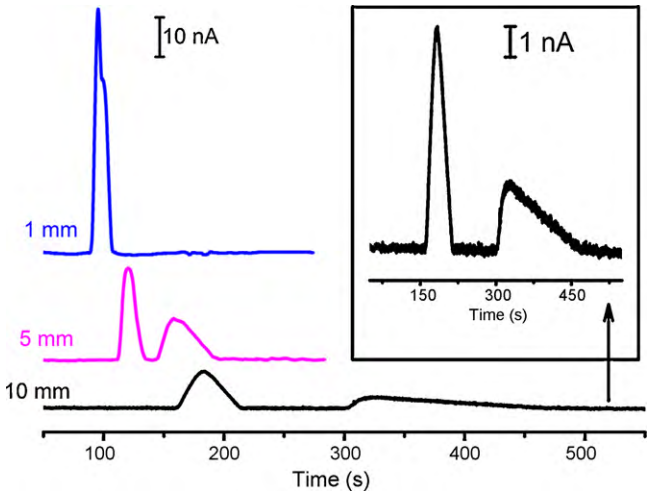

Fig. 4. Effect of packing length of MIP–MNPs in microchannel on enantioseparation of racemic ofloxacin. Electrochromatographic conditions were the same as Table 1 except the packing length.

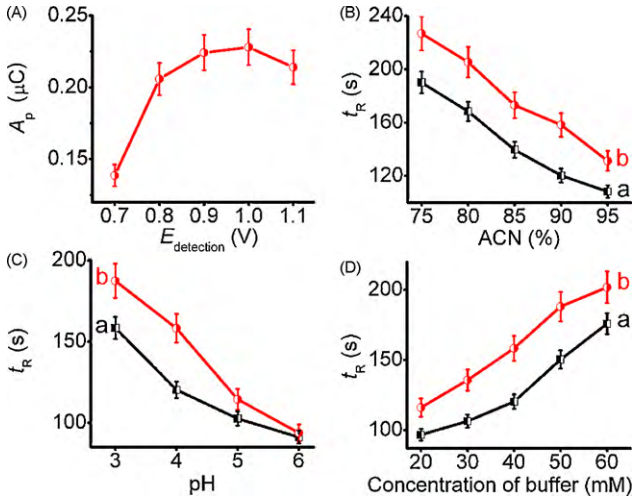

Fig. 5. Effect of (A) detection potential on peak area for 0.1 mM S-ofloxacin, and (B) volume content of ACN, (C) pH and (D) concentration of acetate buffer on retention time of (a) R-ofloxacin and (b) S-ofloxacin at injection voltage of 200 V for 2 s and separation voltage of 1200 V. Electrochromatographic conditions: ACN/40 mM acetate buffer (90/10 (v/v), pH 4.0) as mobile phase and +1.0 V of detection potential. When one parameter changed, the other parameters kept constant.

empty capillary (Fig. 3C), a permeable and homogeneous packing of the MIP–MNPs could be obtained in the MIP–MNPs located capillary (Fig. 3D). The length of the stationary phase could be regulated by changing the magnet length. Thus the separation conditions for chiral drugs could be conveniently optimized. This procedure was apparently easier than the conventional packing techniques, thus the separation efficiency could be optimized by changing conveniently the length of MIP–MNP packing zone. Moreover, except the magnetic field applied region, no adsorption of MIP–MNPs was observed on the inner surface of the microchannel, and the frits were also unnecessary for the preparation of MIP–MNPs–MD.

To evaluate this utility of the packing technique, the enantiomeric separation of racemic ofloxacin was performed at different zone lengths of MIP–MNP packing controlled by the length of the magnet (Fig. 4). The resolution of enantioseparation increased with the increasing packing length from 1 to 10 mm. Although the highest resolution (R_s = 3.18) was obtained at the packing length of 10 mm, the peak tailing for S-ofloxacin was serious with unstable baseline. The sufficient resolution could be achieved within 195 s at 5-mm packing length. So, the packing length of 5 mm was selected in the following experiment.

3.4. Detection potential

Although the analytes have nicely UV–vis absorption, amperometric detection was selected due to the excellent sensitivity, selectivity, easy to miniaturization, and low-power requirements [49]. The electrochemical oxidation of S-ofloxacin at the carbon fiber microdisk electrode produced detectable amperometric signal. The detection potential was investigated using ACN/40 mM acetate buffer (90/10 (v/v), pH 4.0) as mobile phase at separation voltage of 1200 V and injection voltage of 200 V for 2 s. When the applied potential was less than +0.7 V, the signal was very low. With the increasing applied potential from +0.7 to +1.0 V, the amperometric response increased, and a sharp increase occurred at the applied potential of +0.7 to +0.8 V (Fig. 5A). When the applied potential was higher than +1.0 V, the oxidation current decreased slightly. Therefore, +1.0 V was used as the optimum detection potential.

3.5. Optimization of mobile phase

The chromatographic parameters such as the volume content of ACN, pH and concentration of acetate buffer in mobile phase were optimized at detection potential of +1.0 V, separation voltage of 1200 V and injection voltage of 200 V for 2 s. The effect of the volume content of ACN on the retention of R- and S-ofloxacin was investigated at the different ratios (v/v) of ACN/40 mM acetate buffer (pH 4.0) with constant buffer concentration. When ACN content changed from 75 to 95%, both the retention times in S-ofloxacin-imprinted MD (S-ofloxacin-MD) decreased due to the increasing electroosmotic flow mobility [46] and the weakening interaction between MIP and these compounds (Fig. 5B). At the ACN content of 90%, the baseline separation could be given in 195 s for ofloxacin enantiomers. Thus ACN content of 90% (v/v) in the mobile phase was selected as the optimal condition for the enantioseparation.

The influence of pH in the range of 3.0–6.0 on the retention of R- and S-ofloxacin using ACN/40 mM acetate buffer (90/10, v/v) was shown in Fig. 5C. With the increasing pH value of the mobile phase from 3.0 to 6.0, both retention times of R- and S-ofloxacin decreased due to the increase in the electroosmotic flow mobility (Fig. 5C). At the pH value of 5.0–6.0, the difference of retention times between two compounds became smaller due to the non-selective interactions between analytes and MIPs at high pH value [46]. Thus the value of pH 4.0 was selected for the preparation of the mobile phase.

Fig. 5D shows the effect of the concentration of acetate buffer (pH 4.0) mixed with ACN (10/90, v/v) on the retention of ofloxacin enantiomers on S-ofloxacin-MD. With the increasing concentration, both retention times of R- and S-ofloxacin increase due to the decreasing electroosmotic flow and elution ability. It is well known that the separation efficiency of capillary electrochromatography can be improved with an increasing buffer concentration. However, too high buffer concentration can cause severe joule heating [34]. Thus 40 mM acetate buffer was chosen to secure good separation efficiency as well as stable baseline without current disturbances.

3.6. Sampling conditions and separation voltage

The designed MD allowed injecting various volumes of sample by changing the sampling time or voltage. High sampling voltage usually resulted in high injection current to induce an unstable baseline and low separation efficiency. The ultranarrow sampling fracture [38] could produce a fast sampling speed at relatively low injection voltage, which allowed a short sampling time. When the injection voltage was lower than 50 V, one long sampling time was need to obtain a detectable sample plug, resulting in serious

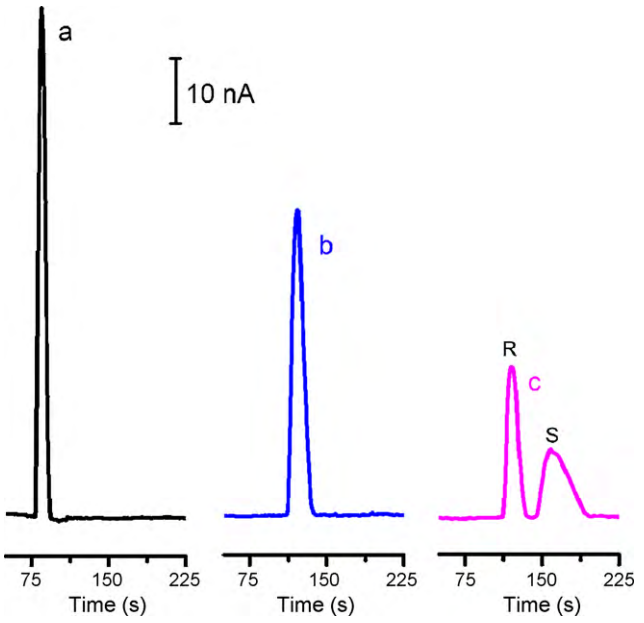

Fig. 6. Electropherograms of racemic ofloxacin with (a) the MD integrated with empty microchannel, (b) NIP–MNPs–MD and (c) MIP–MNPs–MD. Electrochromatographic conditions were the same as Table 1.

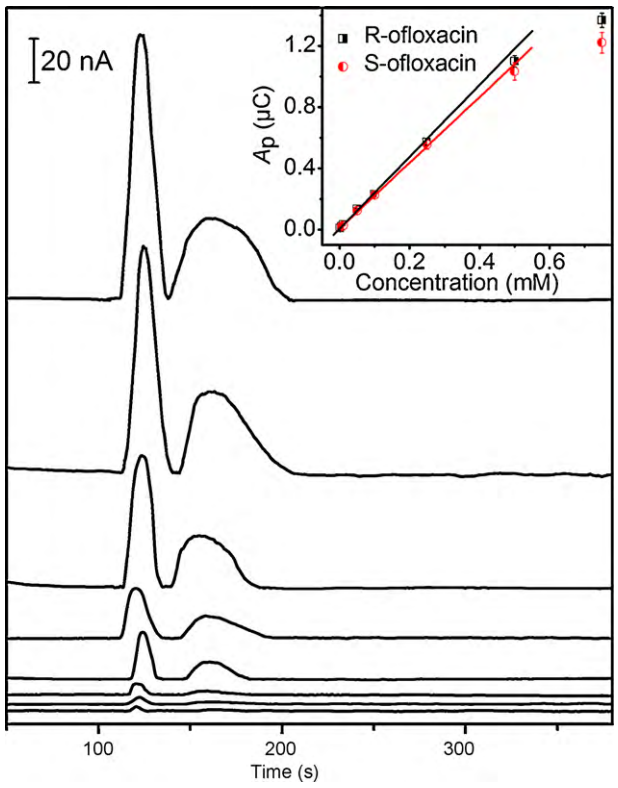

Fig. 7. Electropherograms of two ofloxacin enantiomers at the individual concentrations of 1, 5, 10, 50, 100, 250, 500 and 750 μM from bottom to top. Inset: calibration curves for R-ofloxacin and S-ofloxacin detection. Electrochromatographic conditions were the same as Table 1.

sample broadening and low separation efficiency. The short time favored depressing the diffusion of the analytes during the sampling process for avoiding the broadening of the sample zone. At the sampling voltage of 200 V, with the increase of sampling time the signal increased and trended to a constant peak current after 2 s. Thus, an optimum injection voltage of 200 V at the injection time of 2 s was selected for obtaining high separation efficiency and appropriate detection sensitivity.

At the separation voltages more than 1400 V, baseline drift appeared in the separation process. With the decrease of separation voltage from 1200 to 800 V, the separation time lengthened from 158 to 223 s, while the resolution decreased due to the broadening of signal. At 1200 V, baseline separation of ofloxacin enantiomers was successfully acquired within 195 s on the S-ofloxacin-MD. The separation time obtained from the resulting MIP–MNPs–MD was much shorter than 10 min in conventional molecularly imprinted capillary electrochromatographic analysis [34].

3.7. Enantioseparation and detection of racemic ofloxacin

Prior to microchip electrochromatographic analysis, the effect of magnetic field on the separation of ofloxacin enantiomers was investigated. The effective electrophoretic mobility and peak width of racemic ofloxacin were identical whether applying the magnetic field or not. Thus, the magnetic field would not affect the separation efficiency under the optimal conditions. The electropherograms of ofloxacin enantiomers on the MD with empty microchannel, NIP–MNPs–MD, and MIP–MNPs–MD were shown in Fig. 6. Both the MD integrated with empty microchannel and the NIP–MNPs–MD could not separate ofloxacin enantiomers (Fig. 6a and b) due to the absence of the recognition sites complementary to the spatial structure of S-ofloxacin. Contrarily, baseline separation was achieved with the resolution of 1.46 on MIP–MNPs–MD (Fig. 6c). This result could be attributed to sufficient recognition sites of MIP–MNPs densely packed in the microchannel for effective recognition of S-ofloxacin. Although the broadening peak was observed, especially the tailing of the imprinted analyte (i.e. S-ofloxacin), due to the unfavorable association and dissociation kinetics of analyte with the MIP stationary phase, which was considered to arise from imprint heterogeneity and slow on-off kinetics [50], the MIP–MNPs–MD could separate the enantiomers with the predetermined elution order by the choice of template molecules used for the molecular imprinting.

The amperometry was employed to detect ofloxacin enantiomers with a carbon fiber microdisk electrode at +1.0 V (vs. Ag/AgCl). The linear ranges were from 1.0 to 500 μM for R-ofloxacin and 5.0 to 500 μM for S-ofloxacin with the relative coefficients of 0.995 and 0.997 and the slopes of 2.35 and 2.15 μC mM^{-1}, respectively (Fig. 7). The detection limits at the ratio of S/N of 3 were 0.4 and 2.0 μM for R- and S-ofloxacin, respectively, which were much lower than 17.5 and 22.2 μM of capillary electrochromatography at the ratio of S/N of 5 for the ofloxacin enantiomers with an open tubular MIP capillary [34]. Although the quantitative results were not good enough to compete with conventional chromatographic methods [36,37], the proposed method showed fast separation and low consumption of reagents and samples.

The relative standard deviations (RSDs) of migration times of R- and S-ofloxacin ($n = 3$) were 1.1 and 1.2% for run-to-run, 2.3 and 2.5% for day-to-day, and 4.3 and 5.6% for chip-to-chip, respectively. The RSDs of peak area (A_p) measured at the racemic ofloxacin concentration of 0.2 mM ($n = 3$) were 1.5 and 2.1% for run-to-run, 3.4 and 5.5% for day-to-day, and 7.2 and 8.3% for chip-to-chip, respectively. These results suggested that the proposed method had good stability and precision, and the MIP–MNPs–MD had good fabrication reproducibility.

4. Conclusions

A MD integrated with MIP–MNPs as magnetically tunable stationary phase was designed for rapid enantioseparation. The MIP–MNPs were synthesized via chemical polymerization on the

surface of MNPs, and provided a permeable and homogeneous packing structure in the microchannel of MD, resulting in high efficient separation. The as-prepared MIP–MNPs could be conveniently localized to the pre-nominated position in the separation channel by applying an external magnetic field. Moreover, the length of the MNP packing zone could be easily varied by changing the magnet length. Under optimal conditions, efficient molecular recognition of ofloxacin enantiomers was achieved in MIP–MNPs–MD, leading to baseline enantioseparation and good reproducibility and detection precision. Compared with conventional enantioselective separation, the designed MIP–MNPs–MD could use a magnet field to tune the length of MIP–MNPs packing zone for quick enantioscreening of different kinds of chiral compounds.

Acknowledgements

We gratefully acknowledge the financial support of the National Basic Research Program of China (Grant 2010CB732400) from the Ministry of S&T and the National Natural Science Foundation of China (Grant 20821063, 20835006, 90713015 and 20875044).

References

[1] J. Tan, H.F. Wang, X.P. Yan, Anal. Chem. 81 (2009) 5273.
[2] R.Z. Ouyang, J.P. Lei, H.X. Ju, Y.D. Xue, Adv. Funct. Mater. 17 (2007) 3223.
[3] D. Lakshmi, A. Bossi, M.J. Whitcombe, I. Chianella, S.A. Fowler, S. Subrahmanyam, E.V. Piletska, S.A. Piletsky, Anal. Chem. 81 (2009) 3576.
[4] A. Pietrzyk, S. Suriyanarayanan, W. Kutner, R. Chitta, F. D'Souza, Anal. Chem. 81 (2009) 2633.
[5] H.F. Wang, Y. He, T.R. Ji, X.P. Yan, Anal. Chem. 81 (2009) 1615.
[6] J.Q. Liu, G. Wullf, J. Am. Chem. Soc. 130 (2008) 8044.
[7] Z.G. Xu, Y.F. Hu, Y.L. Hu, G.K. Li, J. Chromatogr. A 1217 (2010) 3612.
[8] Y.P. Huang, Z.S. Liu, C. Zheng, R.Y. Gao, Electrophoresis 30 (2009) 155.
[9] P. Spégel, L. Schweitz, S. Nilsson, Anal. Chem. 75 (2003) 6608.
[10] H.F. Wang, Y.Z. Zhu, X.P. Yan, R.Y. Gao, J.Y. Zheng, Adv. Mater. 18 (2006) 3266.
[11] L. Schweitz, P. Spégel, S. Nilsson, Analyst 125 (2000) 1899.
[12] N.M. Maier, W. Lindner, Anal. Bioanal. Chem. 389 (2007) 377.
[13] C. Nilsson, S. Birnbaum, S. Nilsson, J. Chromatogr. A 1168 (2007) 212.
[14] J.Z. Hilt, M.E. Byrne, Adv. Drug Deliv. Rev. 56 (2004) 1599.
[15] R. Suedee, T. Srichana, T. Rattananont, Drug Deliv. 9 (2002) 19.
[16] S. Tokonami, H. Shiigi, T. Nagaoka, Anal. Chim. Acta 641 (2009) 7.
[17] D.M. Gao, Z.P. Zhang, M.H. Wu, C.G. Xie, G.J. Guan, D.P. Wang, J. Am. Chem. Soc. 129 (2007) 7859.
[18] S.R. Carter, S. Rimmer, Adv. Funct. Mater. 14 (2004) 553.
[19] C.D. Ki, J.Y. Chang, Macromolecules 39 (2006) 3415.
[20] H.H. Yang, S.Q. Zhang, F. Tan, Z.X. Zhuang, X.R. Wang, J. Am. Chem. Soc. 127 (2005) 1378.
[21] C.G. Xie, B.H. Liu, Z.Y. Wang, D.M. Gao, G.J. Guan, Z.P. Zhang, Anal. Chem. 80 (2008) 437.
[22] H.J. Wang, W.H. Zhou, X.F. Yin, Z.X. Zhuang, H.H. Yang, X.R. Wang, J. Am. Chem. Soc. 128 (2006) 15954.
[23] W.H. Zhou, C.H. Lu, X.C. Guo, F.R. Chen, H.H. Yang, X.R. Wang, J. Mater. Chem. 20 (2010) 880.
[24] C.J. Tan, Y.W. Tong, Anal. Chem. 79 (2007) 299.
[25] Y. Zhang, R.J. Liu, Y.L. Hu, G.K. Li, Anal. Chem. 81 (2009) 967.
[26] L.G. Chen, J. Liu, Q.L. Zeng, H. Wang, A.M. Yu, H.Q. Zhang, L. Ding, J. Chromatogr. A 1216 (2009) 3710.
[27] M.A. Hayes, N.A. Polson, A.N. Phayre, A.A. Garcia, Anal. Chem. 73 (2001) 5896.
[28] V. Sivagnanam, B. Song, C. Vandevyver, M.A.M. Gijs, Anal. Chem. 81 (2009) 6509.
[29] Y.K. Hahn, Z.W. Jin, J.H. Kang, E.K. Oh, M.K. Han, H.S. Kim, J.T. Jang, J.H. Lee, J.W. Cheon, S.H. Kim, H.S. Park, J.K. Park, Anal. Chem. 79 (2007) 2214.
[30] K.S. Kim, J.K. Park, Lab Chip 5 (2005) 657.
[31] R.S. Sista, A.E. Eckhardt, V. Srinivasan, M.G. Pollack, S. Palanki, V.K. Pamula, Lab Chip 8 (2008) 2188.
[32] J.W. Choi, K.W. Oh, J.H. Thomas, W.R. Heineman, H.B. Halsall, J.H. Nevin, A.J. Helmicki, H.T. Henderson, C.H. Ahn, Lab Chip 2 (2002) 27.
[33] P. Qu, J.P. Lei, R.Z. Ouyang, H.X. Ju, Anal. Chem. 81 (2009) 9651.
[34] S.A. Zaidi, K.M. Han, S.S. Kim, D.G. Hwang, W.J. Cheong, J. Sep. Sci. 32 (2009) 996.
[35] I. Hayakawa, S. Atarashi, S. Yokohama, M. Imamura, K.I. Sakano, M. Furukawa, Antimicrob. Agents Chemother. 29 (1986) 163.
[36] H.Y. Yan, K.H. Row, Anal. Chim. Acta 584 (2007) 160.
[37] C. Horstkötter, G. Blaschke, J. Chromatogr. B 754 (2001) 169.
[38] C. Zhai, W. Qiang, J.P. Lei, H.X. Ju, Electrophoresis 30 (2009) 1490.
[39] Y.C. Wang, Z.C. Zhang, L. Zhang, F. Li, L. Chen, Q.H. Wan, Anal. Chem. 79 (2007) 5082.
[40] Y. Okamoto, Y. Ikawa, F. Kitagawa, K. Otsuka, J. Chromatogr. A 1143 (2007) 264.
[41] C. Zhai, C. Li, W. Qiang, J.P. Lei, X.D. Yu, H.X. Ju, Anal. Chem. 79 (2007) 9427.
[42] W.Y. Yan, R.Y. Gao, Z.C. Zhang, Q.S. Wang, C.V. Jiang, C. Yan, J. Sep. Sci. 26 (2003) 555.
[43] C. Yu, O. Ramstrom, K. Mosbach, Anal. Lett. 30 (1997) 2123.
[44] X.W. Kan, Z.R. Geng, Y. Zhao, Z.L. Wang, J.J. Zhu, Nanotechnology 20 (2009) 16501.
[45] K. Yoshimatsu, K. Reimhult, A. Krozer, K. Mosbach, K. Sode, L. Ye, Anal. Chim. Acta 584 (2007) 112.
[46] Z.S. Liu, Y.L. Xu, C. Yan, R.Y. Gao, J. Chromatogr. A 1087 (2005) 20.
[47] Z.J. Tan, V.T. Remcho, Electrophoresis 19 (1998) 2055.
[48] J.J. Ou, X. Li, S. Feng, J. Dong, X.L. Dong, L. Kong, M.L. Ye, H.F. Zou, Anal. Chem. 79 (2007) 639.
[49] J. Wang, S. Mannino, C. Camera, M.P. Chatrathi, M. Scampicchio, J. Zima, J. Chromatogr. A 1091 (2005) 177.
[50] L. Schweitz, Anal. Chem. 74 (2002) 1192.